



**Intracellular uptake of EGCG-loaded deformable controlled release liposomes for skin cancer**

Journal:	<i>Journal of Liposome Research</i>
Manuscript ID	Draft
Manuscript Type:	Original Paper
Date Submitted by the Author:	n/a
Complete List of Authors:	Marwah, Mandeep; Aston University, Pharmacy Perrie, Yvonne; University of Strathclyde, Pharmacy and Biomedical Sciences Badhan, Raj; Aston University, Pharmacy Lowry, Deborah; University of Ulster, Pharmacy
Keywords:	Skin cancer, deformable liposomes, dermal release, controlled release, elastic liposomes

SCHOLARONE™  
Manuscripts

1  
2  
3  
4  
5  
6  
7  
8  
9  
10  
11  
12  
13  
14  
15  
16  
17  
18  
19  
20  
21  
22  
23  
24  
25  
26  
27  
28  
29  
30  
31  
32  
33  
34  
35  
36  
37  
38  
39  
40  
41  
42  
43  
44  
45  
46  
47  
48  
49  
50  
51  
52  
53  
54  
55  
56  
57  
58  
59  
60

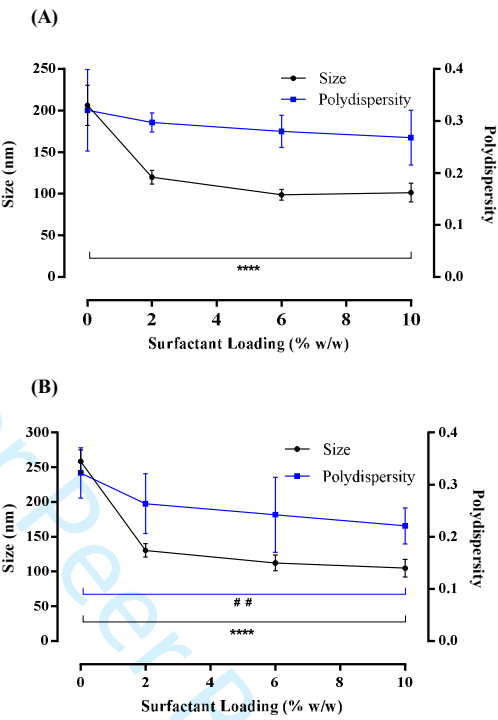


**Fig. 1** Liposome size distribution and polydispersity of ‘empty’ and EGCG loaded liposomes

Liposome size distribution and polydispersity, determined by DLS, comparing (A) ‘empty’ and (B) EGCG loaded formulations with Tween 20 (0-10 % w/w). Liposomes were prepared by the dry film hydration method and EGCG added during the lipid mixing stage. Data represents mean  $\pm$  SD. n=3 independent batches. \*\*\*\* indicates statistical comparison between the size of liposome formulations with a  $P \leq 0.0001$ . ## indicates statistical comparison between the polydispersity of liposome formulations with a  $P \leq 0.01$ .

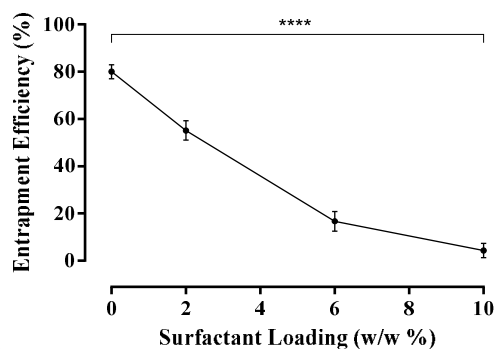


**Fig. 2** Entrapment efficiency of EGCG in liposomes formulated with 0-10% w/w Tween 20

Entrapment efficiency (%) of EGCG in liposomes formulated with varying amounts of Tween 20 (0-10% w/w). Data represents mean  $\pm$  SD, n=3 independent batches. \*\*\*\* indicates statistical comparison between the entrapment efficiency of liposome formulations with a  $P \leq 0.0001$ .

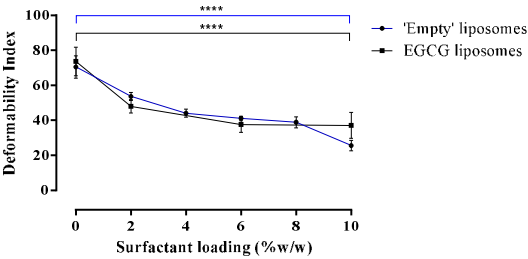


**Fig. 3** Deformability index for ‘empty’ and EGCG loaded liposomes

Deformability index following extrusion through 50 nm membranes for ‘empty’ and EGCG loaded liposomes with increasing surfactant loading up to a maximum of 10% w/w. Liposomes were prepared adapting the dry film method adding the surfactant and adding EGCG during the lipid mixing stage. The preparation was vortexed and then extruded through the membranes. Data represents mean ± SD. n=3 independent batches. \*\*\*\* indicates statistical comparison between the DI of liposome formulations with a  $P \leq 0.0001$ .

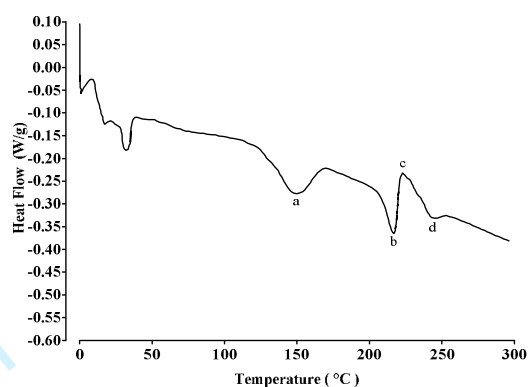


**Fig. 4** Differential scanning calorimetry scan of EGCG

All experimental runs commenced at an initial temperature of 0 °C with a scan rate of 10 °C/min to 300 °C. Peak a and b are related to the epimer of EGCG, GCG. Peak c represents the glass transition temperature ( $T_g$ ) of EGCG was at 220 °C and the melting point ( $T_m$ ) of EGCG was at 245 °C.

1  
2  
3  
4  
5  
6  
7  
8  
9  
10  
11  
12  
13  
14  
15  
16  
17  
18  
19  
20  
21  
22  
23  
24  
25  
26  
27  
28  
29  
30  
31  
32  
33  
34  
35  
36  
37  
38  
39  
40  
41  
42  
43  
44  
45  
46  
47  
48  
49  
50  
51  
52  
53  
54  
55  
56  
57  
58  
59  
60

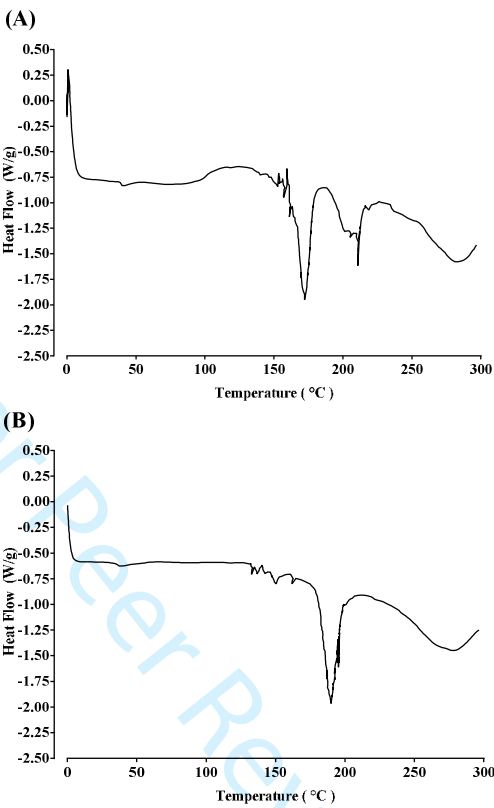


**Fig. 5** Differential scanning calorimetry analysis scans of PC, cholesterol and Tween 20 and EGCG blends

DSC analysis scans of (A) PC, cholesterol and Tween 20 blend and (B) PC, cholesterol, Tween 20 and EGCG blend. The  $T_m$  of the lipid mixture is 172 °C, and upon addition of EGCG, the  $T_m$  was 191 °C. All experimental runs started at an initial temperature of 0 °C, purged under nitrogen gas, with a scan rate of 10 °C/min to 300 °C.

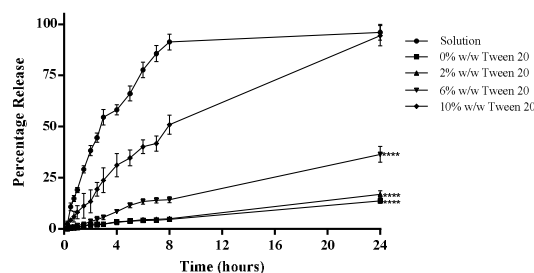


**Fig. 6** *In-vitro* percentage EGCG cumulative release profiles from solution and liposomal formulations

EGCG release profiles from solution and liposomes formulated with 0, 2, 6 or 10 % w/w Tween 20 over 24 hours. Liposomes were prepared adapting the dry film method adding the surfactant and EGCG during the lipid mixing stage. A diffusion cell dialysis system was used to evaluate *in-vitro* drug release. Data represents mean  $\pm$  SD. n=3 independent batches. \*\*\*\* indicates statistical comparison between the EGCG release of liposome formulations with a  $P \leq 0.0001$ .

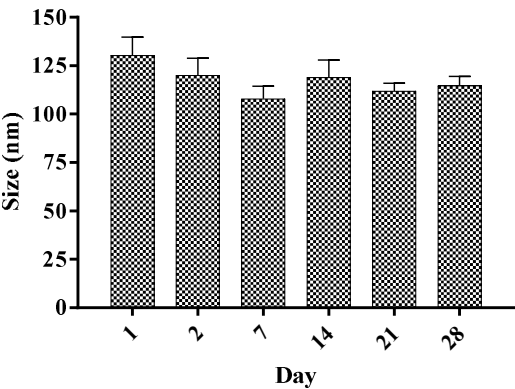


**Fig. 7** Stability of EGCG loaded liposomes as determined by size

Size of EGCG loaded liposomes formulated with 0-10% w/w Tween 20, using DLS, formulated with up to 10% w/w Tween 20 measured on various days (1, 7, 14, 21 and 28). Data represents mean  $\pm$  SD. n=6 independent batches.

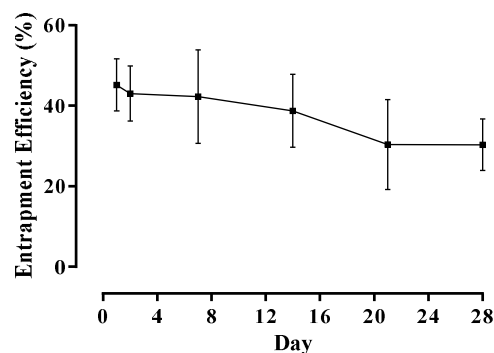


**Fig. 8** Liposome encapsulation efficiency for EGCG

Liposome encapsulation efficiency for EGCG in liposomes formulated with 2 % w/w Tween 20 liposomes over 28 days. Liposomes were prepared adapting the dry film method adding the surfactant and drug during the lipid mixing stage. The preparation was then washed via centrifugation. The quantity of EGCG in supernatant over 28 days was then analysed by HPLC coupled with UV detection to assess liposome stability. Data represents mean  $\pm$  SD. n=6 independent batches.

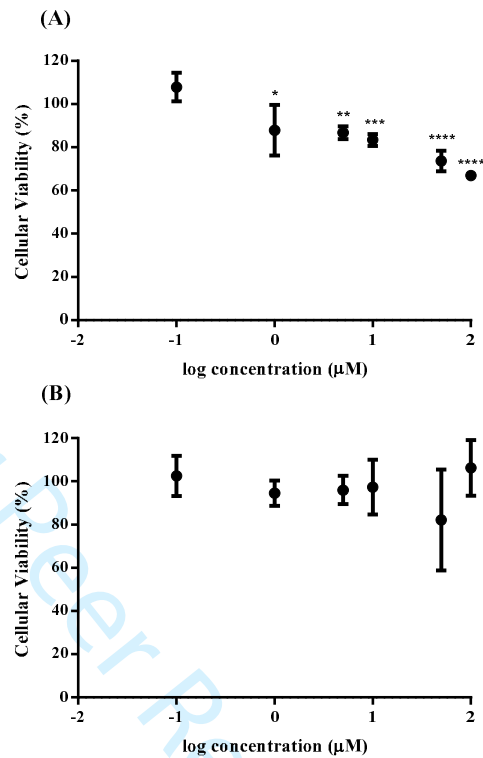


**Fig. 9** Cellular toxicity of EGCG

HDFa (A) and HaCat (B) cells were grown on a 96-well plate at a density of  $50 \times 10^3$  cells per well and exposed to various concentrations of EGCG (0.01-100  $\mu\text{M}$ ) for 24 hours. Thereafter 25  $\mu\text{L}$  of a 12.5:1 parts mixture of XTT to menadione was added each well. Plates were incubated for 3 hours at  $37^\circ\text{C}$  and the absorbance read at 450 nm. Data is reported as mean  $\pm$ SD with 6 replicates per compound in at 3 independent experiments. \*\*\*\*, \*\*\*, \*\*, \* indicates statistical comparison between the entrapment efficiency of liposome formulations with a  $P \leq 0.0001$ , 0.001, 0.01 and 0.05 respectively.

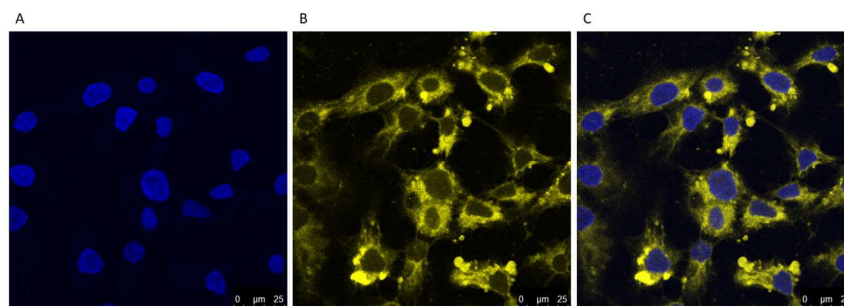


**Fig. 10** Localisation of DiIc labelled liposomes loaded with EGCG and 2% w/w Tween 20 in HaCat cells

Cells were grown on the coverslips for 2 days. Cell nuclei were visualised using (A) DAPI (Blue). Liposomes were formulated with DiIc for visualisation (B) (yellow). Liposome localisation within the cell is shown in the merged image (C).

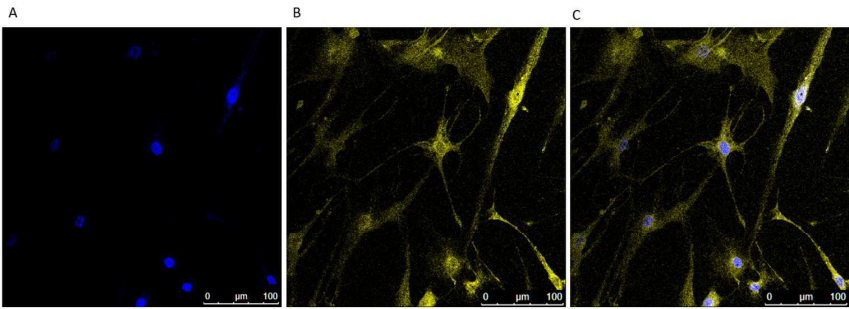


**Fig. 11** Localisation of DiIC labelled liposomes loaded with EGCG and 2% w/w Tween 20 in HDFa cells

Cells were grown on the coverslips for 2 days. Cell nuclei were visualised using (A) DAPI (Blue). Liposomes were formulated with DiIC for visualisation (B) (yellow). Liposome localisation within the cell is shown in the merged image (C).

- 1
- 2
- 3
- 4 1 Intracellular uptake of EGCG-loaded deformable controlled release liposomes for skin
- 5
- 6 2 cancer
- 7
- 8 3
- 9
- 10 4
- 11
- 12
- 13
- 14
- 15
- 16
- 17
- 18
- 19
- 20
- 21
- 22
- 23
- 24
- 25
- 26
- 27
- 28
- 29
- 30
- 31
- 32
- 33
- 34
- 35
- 36
- 37
- 38
- 39
- 40
- 41
- 42
- 43
- 44
- 45
- 46
- 47
- 48
- 49
- 50
- 51
- 52
- 53
- 54
- 55
- 56
- 57
- 58
- 59
- 60

For Peer Review Only

**ABSTRACT**

Caucasian population groups have a higher propensity to develop skin cancer, and associated clinical interventions often present substantial financial burden on healthcare services. Conventional treatments are often not suitable for all patient groups as a result of poor efficacy and toxicity profiles. The primary objective of this study was to develop a deformable liposomal formulation, the properties of which being dictated by the surfactant Tween 20, for the dermal cellular delivery of epigallocatechin gallate (EGCG), a compound possessing antineoplastic properties. Results demonstrated a significant decrease in liposome deformability index ( $73.66 \pm 8.14$  to  $37.06 \pm 7.41$ ) as Tween 20 loading increased from 0 to 10 % w/w, indicating an increase in elasticity. EGCG release over 24-hours demonstrated Tween 20 directly incorporation increased release from  $13.7 \% \pm 1.1 \%$  to  $94.4 \% \pm 4.9 \%$  (for 0 and 10 % w/w Tween 20 respectively). Finally, we demonstrated DilC-loaded deformable liposomes were localised intracellularly within human dermal fibroblast and keratinocyte cells within 2-hours. Thus it was evident deformable liposomes are useful in enhancing drug penetration into dermal cells and would be useful in developing a controlled-release formulation.

**KEYWORDS:** Skin cancer; deformable liposomes; dermal release; controlled release; elastic liposomes

## 1. Introduction

Skin cancer is emerging as an increasing public health problem particularly in developed countries [1]. Currently, 2-3 million non-melanoma skin cancers and 132,000 melanoma skin cancers occur globally each year [2]. The large number of cases diagnosed present as a substantial burden to healthcare services [3, 4, 2]. Despite the fact that the majority of skin cancers are treatable, malignant forms of the cancer results in over 9,000 deaths annually worldwide [5]. Current treatment approaches are limited to local surgery to remove the tumour in addition to topical treatments with cream formulations. However, surgical removal may not be suitable for all patients whilst topical therapies are often linked with poor patient compliance stemming from high dose frequency requirements and unpleasant side effects [6]. In addition, topical treatments may cause skin irritation, weeping, cracking and blistering causing discomfort and pain [7-9].

Strategies for cancer management are focused on chemoprevention and chemoprotection. Existing anticancer agents often demonstrate poor safety profiles in addition to unpleasant side effect profiles, and there is an urgent need for novel agents which are both efficacious and possess a limited toxicity profile to non-malignant dermal tissue [10-12]. One group of compounds that have gained interest recently as novel candidates for this purpose are flavonoids, naturally occurring chemicals abundantly expressed in food and drink, and in particular the green tea catechin, epigallocatechin gallatein (EGCG) which is increasingly being exploited for its chemoprevention properties [13-15]. EGCG has been found to affect specific biological processes that could be exploited as targets for the prevention and treatment of cancer [16], and has been demonstrated to possess properties associated with the induction of apoptosis [17], promotion of cell growth arrest by altering the expression of cell cycle regulatory proteins [17], activation of killer caspases and the

52 suppression of oncogenic transcription factors [18, 19, 15] and pluripotency maintaining  
53 factors [20]. However, the application of naturally occurring compounds as  
54 chemopreventative and chemoprotective strategies for skin cancer management has so far  
55 been received with limited success and this may be largely due to inefficient delivery systems  
56 and limited oral bioavailability of promising agents [21-23]. Consequently, to achieve  
57 maximum clinical efficacy, novel approaches are required to enhance compound  
58 bioavailability, of which dermal delivery is particularly promising.

59 The principle function of mammalian skin is to offer protection from environmental  
60 chemicals and xenobiotics [24]. The penetration of drugs across the skin is significantly  
61 inhibited by the skin's inherent barrier properties [25] thus there is a need to develop carrier  
62 systems to enhance penetrability. To fulfil this goal, when applied topically nanoparticle  
63 mediated delivery systems (e.g. microemulsions, liposomes, ethosomes, deformable  
64 liposomes and solid lipid nanoparticles), would benefit the direct dermal delivery of  
65 compounds across the stratum corneum [26-28]. Additionally, such nano-scale structures are  
66 capable of improving drug loading, enhancing systemic bioavailability, imparting a sustained  
67 release profile and allowing targeted drug delivery [29, 30]. Furthermore, the topical  
68 application of such carriers reduces the incidence of undesirable side effects arising from  
69 systemic administration and enhances systemic absorption of drugs after topical application  
70 with permeation enhancers which irreversibly disrupt the stratum corneum [29, 30].  
71 Controversy however surrounds the use of conventional liposomes due to their large size  
72 preventing skin penetration [31, 28, 32, 33], Gregor Cevc [34] demonstrated that  
73 modification of the chemical composition of the lipid bilayer so as to decrease its Young's  
74 modulus resulted in the formation of deformable liposomes. These are able to gain access to  
75 the viable epidermis by overcoming the physical constraints imposed by the stratum corneum  
76 by diminishing the membrane elastic energy required for the liposome to deform and fit

through an aperture size smaller than their original diameter following which reforming to their original shape [35, 36, 31]. By being able to change shape and volume at minimal energetic cost, these structures may penetrate across hydrophilic pathways of intact skin [37, 36]. Deformable liposomes often include additional components designed to make the membrane more liable to deformation and these are termed edge-activators, typically including surfactants such as Tweens, bile salts and Myrj [38]. The inclusion of this extra component destabilises the vesicle bilayers by reducing the amount of energy required to expand the interface allowing the liposome to become more elastic thus increasing the flux across the skin [38-40].

The primary aim of this study was to develop and characterise a deformable controlled release liposome formulation for targeting toward intracellular uptake into dermal cells. The objectives of the study were therefore to: (i) assess the impact of the edge-activator Tween 20 on liposomal formulation size; (ii) characterise resultant liposomes vesicle size, surface charge and encapsulation efficiency; (iii) quantify deformability of resultant liposomes using a deformability index (DI); (iv) assess release of EGCG; (v) assess the deformable liposome stability. ; (vi) assess cellular toxicity of EGCG and (vii) assess intracellular uptake in human dermal fibroblast and keratinocyte cells.

## 2. Materials and methods

### 2.1 Materials

Phosphatidylcholine (PC) was obtained from Avanti Polar Lipids. Cholesterol, Tween 20 and EGCG were obtained from Sigma-Aldrich. All other reagents including methanol and chloroform were obtained from Fisher Scientific. Ultrapure water was obtained from a Milli-

Q purification system (Millipore, Billerica, MA, US). Human dermal fibroblasts (HDFa) isolated from adult skin and all cell culture reagents (Medium 106 and low serum growth supplement (LSGS) kit containing supplemented medium containing foetal bovine serum, 2 % v/v, hydrocortisone 1 µg/mL, human epidermal growth factor, 10 ng/mL, basic fibroblast growth factor, 3 ng/mL, heparin, 10 µg/mL; DMEM media supplemented with 1 % L-glutamine, 10 % FBS, 1 % Penicillin Streptomycin and 0.25% amphotericin) were obtained from Life technologies (Carlsbad, California, US). Immortalized human keratinocytes (HaCat) cells were a kind gift from Dr Andrew Sanders (Cardiff China Medical Research Collaborative, Cardiff University, Henry Wellcome Building, Heath Park, Cardiff, CF14 4XN).

## 2.2 Methods

### 2.2.1 Preparation of deformable liposomes with or without an edge activator

Liposomes were prepared by adapting the film hydration method established by Bangham *et al.*, (1965) [41]. PC and cholesterol (16:8 µM) were dispersed in an organic solvent mixture consisting of chloroform and methanol in a 9:1 ratio in a round bottomed flask [40, 38, 26, 42, 41]. Subsequently, the organic solvent was removed by rotary evaporation for 5 minutes at 35 °C, followed by purging with nitrogen gas. The resultant dry film residue was hydrated by the addition of 4 mL water containing edge activator (up to 10% w/w of the formulation) and 1 mg of EGCG at a temperature above the transition temperature of the phospholipid (between -7 to -15°C) [43] and vortexed for 5 minutes to form multilamellar vesicles (MLV). The resulting particles were extruded 21 times through 100-nm diameter polycarbonate membranes, using an Avanti Mini Extruder to produce unilamellar vesicles. The formed liposomes were equilibrated for 30 min above their transition temperatures (-15°C) before being subjected to further characterisation [44, 45, 43].

124

125 *2.2.2 Deformable liposome characterisation*

126 The mean particle size and the polydispersity index (measurement of the level of  
127 homogeneity of particle sizes) of liposomes were measured by dynamic light scattering  
128 (DLS) using a Zetaplus (Brookhaven Instruments) following dilution with distilled water (1:4  
129 ratio) to ensure intensity adjustment. A polydispersity value of  $< 0.2$  indicates a homogenous  
130 vesicle population, while polydispersity of  $> 0.3$  indicates heterogeneity [46]. The particle  
131 charge was quantified as zeta potential ( $\zeta$ ). Zeta potential was determined by photon  
132 correlation spectroscopy using a Zetaplus (Brookhaven Instruments). The samples were  
133 diluted three-fold and assessed in triplicate.

134 *2.2.3 HPLC-UV detection of EGCG*

135 Detection of EGCG was assessed using reverse phase HPLC methodology. A Waters  
136 Alliance separation module HPLC with UV detection was utilised at an operating wavelength  
137 of 275 nm [47] with a Waters X select column (5  $\mu$ m C18 4.6 x 150 mm), with a 10  $\mu$ L  
138 injection volume. The mobile phase comprised of a 70:30 ratio of 0.1% TFA in water to  
139 methanol at a flow rate of 1 mL/min. Stock solutions and standard solutions of EGCG were  
140 prepared with both water and ethanol ranging from 0.5-500  $\mu$ g/mL. A final A calibration  
141 curve with an  $R^2$  of 0.997 and linear equation of  $y = 1 \times 10^7 \cdot x$  was obtained.

142 *2.2.4 Entrapment efficiency of EGCG*

143 The entrapment efficiency of EGCG loaded deformable liposomes was determined by  
144 centrifuging samples and quantifying the EGCG in the supernatant. Samples were centrifuged  
145 at 18,000 rpm for 30 min at 4°C in an Optima<sup>™</sup> MAX-XP ultracentrifuge to separate the

incorporated drug from the free drug. The supernatant was then analysed using HPLC to determine the encapsulation efficiency of EGCG in liposomal formulations (Equation 1):

$$E = \frac{D_t - D_s}{D_t} \times 100\% \quad (1)$$

where  $E$  is the encapsulation efficiency (%),  $D_t$  is the total drug content (mg) and  $D_s$  is drug content in supernatant (mg).

#### 2.2.5 Assessment of liposomal deformability

To assess the deformability of formulated liposomes, a liposome suspension (6 mL) consisting of a 16:8 micromolar ratio of PC to cholesterol formulated with up to 10% w/w of Tween 20 solution (diluted 3 fold), was passed through a polycarbonate filter of 50 nm pore size using a syringe driver (Cole Parmer, UK) set at 0.6 mL/min for 10 min. The mean particle size and the polydispersity index of liposomes were subsequently quantified by DLS, before and after filtration, to assess the ability of formulated liposomes to regain their size after having been forced through a pore size smaller than their original diameter. The deformability was quantified through the calculation of a deformability index (equation 2) [32]:

$$D = 100 - \frac{L_e}{L} \times 100 \quad (2)$$

where  $D$  is deformability,  $L_e$  is size of extruded liposomes (nm),  $L$  is size of liposomes (nm) prior to extrusion.

#### 2.2.6 Differential scanning calorimetry of EGCG and EGCG lipid blends

To assess thermal characteristics of materials including melting temperatures, phase transitions and heat capacity changes of liposomes, EGCG and ratios of lipid, surfactant and

1  
2  
3 167 drug mixtures corresponding to that of the liposome formulation, were analysed in the solid  
4  
5 168 state using a TA Instruments Q200 Thermal Analysis Differential scanning calorimetry  
6  
7 169 (DSC). 3 mg of EGCG was weighed into T-Zero aluminium pans and then hermetically  
8  
9 170 sealed. All experimental runs commenced at an initial temperature of 0°C, purged under  
10  
11 171 nitrogen gas, with a scan rate of 10°C/min to 300°C.

#### 12 13 14 172 2.2.7 *In-vitro EGCG release studies*

15  
16  
17 173 To assess the impact of inclusion of Tween 20 on EGCG from liposomal formulations, a  
18  
19 174 side—by-side diffusion cell (PermeGear diffusion cell, Hellertown, USA) was maintained at  
20  
21 175 35 °C. Release was assessed over a 24 hour period from an EGCG aqueous solution (0.1  
22  
23 176 mg/mL) and EGCG-loaded liposomes (final loading for liposomes formulated with 0, 2, 6  
24  
25 177 and 10 % w/w Tween 20 was 0.80, 0.55, 0.17 and 0.04 mg/mL respectively). 10 mL of each  
26  
27 178 formulation was placed into the donor side of the diffusion cell and release across a 50 nm  
28  
29 179 membrane (Whatman®) into the receiver side containing 100 mL of dermal dissolution  
30  
31 180 media with a stirrer was measured. The release media was sampled with volume replacement  
32  
33 181 (0.5 mL) over 24 hours and analysed using HPLC-UV quantification.

#### 34 35 36 182 2.2.8 *In-vitro drug release kinetics*

37  
38  
39 183 Several kinetic drug release mathematical models were used to assess drug release from the  
40  
41 184 formulations. The best-fit to the mathematical models described below confirmed the  
42  
43 185 appropriate release kinetics:

44  
45  
46 186 *Zero order model:*  $\frac{M_t}{M_\infty} = k_0 \cdot t$  (3)

47  
48  
49 187 where  $M_t/M_\infty$  is the drug fraction released at time  $t$  and  $k_0$  is the zero-order release constant.

50  
51  
52 188 *First order model:*  $\frac{M_t}{M_\infty} = 1 - e^{-k_1 t}$  (4)

189 where  $M_t/M_\infty$  is the drug fraction released at time  $t$  and  $k_I$  is the first-order release constant.

$$190 \text{ Higuchi model: } \frac{M_t}{M_\infty} = k_H \cdot t^{\frac{1}{2}} \quad (5)$$

191 where  $M_t/M_\infty$  is the drug fraction released at time  $t$  and  $k_H$  is the Higuchi constant.

$$192 \text{ Korsmeyer-Peppas Model: } \frac{C_t}{C} = Kt^n \quad (6)$$

193 where  $C_t/C$  is fraction of drug released at time  $t$ ,  $k$  is the release rate constant. The value of  $n$   
 194 is valuable in understanding drug release mechanisms. When  $n \leq 0.45$  drug release is  
 195 diffusion controlled and can be referred to as 'Fickian' diffusion and when  $n > 0.89$  the  
 196 diffusion is indicative of erosion controlled drug release or class-II kinetics. For situations  
 197 where  $0.45 < n \leq 0.89$  the diffusion is a complex mixture of both processes and often termed  
 198 anomalous transport. In all cases this is based on the assumption of release from a cylinder  
 199 and applied to cumulative release rates  $< 60\%$  [48]

200 Mathematical models to assess release kinetics were fit using Microsoft Excel<sup>®</sup>. Zero order,  
 201 first order, Higuchi and Korsmeyer-Peppas release profiles were applied to release from drug  
 202 solution and drug loaded liposome solution following which regression analysis techniques  
 203 were employed to determine the probable drug-release. The release kinetic model displaying  
 204 the highest  $r^2$  metric ( $\geq 0.95$ ) was determined to be the mechanism, by which release occurred.

#### 205 2.2.9 Liposome stability

206 The stability of liposomes was determined, as prepared in water, through the assessment of  
 207 particle size over a 28-day period, stored in a stability cabinet maintained at  $25 \pm 2^\circ\text{C}$   
 208 (Firlabo, France) at a humidity of  $60\% \pm 5\%$ . Mean particle sizes were determined on days  
 209 1, 2, 7, 14, 21 and 28 by DLS. Furthermore, the encapsulation efficiency of drug loaded  
 210 liposomes was assessed over 4 weeks as detailed in section 2.2.4.

211

212

213 *2.2.10 Development of an in-vitro cellular dermal model*

214 To develop an *in-vitro* system to assess cellular toxicity and cellular uptake of  
215 deformable liposomes into representative human dermal tissue, two dermal cell line were  
216 examined. Human dermal fibroblasts (HDFa) were cultured in Medium 106 supplemented  
217 with low serum growth supplement. Human epidermal keratinocytes (HaCaT) cells were  
218 revived and sustained in high glucose supplemented DMEM media. Media was replaced  
219 every 3 days. At 70-80% confluency, media was discarded and cells detached using  
220 Trypsin/EDTA incubated for 5 min, prior to trypsin neutralisation with 3 mL growth media  
221 and subsequent centrifugation at 1200 rpm for 10 min and resuspension in fresh media prior  
222 to being utilized for subsequent studies

223 *2.2.11 Cellular toxicity of liposomal formulations towards HDFa and HaCat cells*

224 To determine the cytotoxicity profile of EGCG towards HDFa and HaCat cells, a  
225 (2,3-Bis-(2-Methoxy-4-Nitro-5-Sulphophenyl)-2H-Tetrazolium-5-Carboxanilide (XTT) assay  
226 [49] was performed to measure cell viability after exposure to increasing concentrations of  
227 EGCG for 24 hours. Cells were seeded at a density of  $50 \times 10^3$  cells per well into a 96-well  
228 plate and grown for 3 days. Thereafter, media was removed and cells were exposed to 100  $\mu$ L  
229 of 0.1-100  $\mu$ M EGCG and incubated for 24 hours at 37°C. Subsequently, 25  $\mu$ L of a 12.5:1  
230 (XTT: menadione) was added each well and incubated for 3 hours at 37°C prior to the  
231 absorbance being read at 450 nm. Assessment of EGCG toxicity to these cells was conducted  
232 through analysis of changes in XTT absorbance with increasing drug concentration.

233 *2.2.12 Intracellular uptake of deformable liposomes into HDFa and HaCat cells*

Liposomes, both deformable and non-deformable, were formulated with the addition of 0.25 mL of a 0.1 mg/mL DiIc during the lipid mixing stage. Unentrapped DiIc was removed by centrifuging liposomes at 18,000 g for 30 min. Coverslips were coated for 30 min with poly-l-lysine (0.01 % w/v) prior to the addition of cells at a density of  $50 \times 10^3$  cells per coverslip. After 24 hours, DiIc loaded liposomes were diluted with 1 part of supplemented media (as clarified in materials) and were then added to the coverslips and incubated for 2 hours at 37°C.

Thereafter, coverslips were washed and fixed with 4 % w/v paraformaldehyde for 5 minutes at room temperature. Subsequently, coverslips were mounted onto glass slides with the addition of a DAPI-containing mounting media. Cover slips were subsequently analysed in an upright confocal microscope (Leica SP5 TCS II MP) and visualised with a 40× oil immersion objective. Images were acquired using a helium-neon laser at 633 nm to visualise DiIc and a helium–neon laser to visualise DAPI at 461 nm.

#### 2.2.13 Statistical analysis

Unless otherwise stated, all results are presented as mean  $\pm$  standard deviation (SD). Replicates of at least 3 were used for all studies. For multiwell plate assays replicates of 6 were used for each experimental condition with the study replicated 3 times. A one-way ANOVA was used to determine any statistically significant difference between means tested. A post-hoc Tukey's multiple comparisons test was then applied to assess differences between groups. All the calculations were carried out using Graphpad 6 (GraphPad Inc., La Jolla, CA).

### 3. Results and discussion

256 Emerging treatments for cancer management involve chemoprevention and chemoprotection.  
257 Current anticancer agents tend to demonstrate a poor safety profile in addition to possess a  
258 wide range of unpleasant side effects [10-12]. However, phytochemical flavonoids, such as  
259 EGCG, are increasingly being investigated for their chemoprevention properties [13-15].

260 EGCG is a flavonoid found in green tea that possesses cytotoxic effects in cancerous skin  
261 cells and thus may be a potentially viable candidate as a pharmacological anti-cancer agent  
262 [16], given that it has been observed to induce apoptosis in cancer cells without affecting  
263 normal cells [50, 17], in addition to the modulating expression of a number of genes involved  
264 in cell proliferation, cell-cell contact and cell-matrix interactions [51].

265 However, the penetration of drugs across the skin is significantly hindered by the skin's  
266 inherent barrier properties [25]. The use of deformable liposomes to aid dermal cellular  
267 penetrability and uptake may be advantageous in the targeting of neoplastic agents to deeper  
268 skin cellular layers when compared to conventional liposomes which may not be able to  
269 penetrate through the narrow pore of the stratum corneum [39].

270 This focus of this study was to develop EGCG loaded slow release deformable liposomes.  
271 EGCG liposomes were formulated with PC and cholesterol with the inclusion of Tween 20 as  
272 a edge-activator with incorporation of up to 10 % w/w. Liposomal characteristics including  
273 liposome size, charge, encapsulation efficiency, DI, release profile, stability, ceulluar toxicity  
274 and uptake were was assessed.

### 275 ***3.1 Liposome characterisation***

276 The impact of the inclusion of Tween 20 within the liposomal formulation on  
277 liposome characteristics were observed. As the surfactant loading in the bilayer of 'empty'  
278 liposomes increased, liposome diameter decreased from  $206.45 \pm 24.33$  nm for liposomes

formulated with no surfactant to  $101.61 \pm 11.27$  nm for liposomes formulated with 10 % w/w Tween 20 (Figure 1A). As the surfactant loading in the bilayer of EGCG loaded liposomes increased, liposome diameter decreased, from  $258.43 \pm 16.69$  nm for liposomes formulated with no surfactant compared with  $104.95 \pm 12.56$  nm for liposomes formulated with 10 % w/w Tween 20 (Figure 1B). The decrease in size was statistically significant for 'empty' and EGCG loaded liposomes formulated with no surfactant compared with liposomes loaded with 2, 6 and 10 % w/w Tween 20.

[Figure 1 near here]

The inclusion of surfactants into liposome formulations have previously been demonstrated to decrease liposome size when compared to liposomes formulated in the absence of surfactant [26, 32]. This may be as a result of a destabilising effect imparted by the surfactant on the bilayer [52], which results in a greater interaction of the phospholipid bilayer with the aqueous phase. A consequence of this would then be the overall formation of liposomes with a smaller diameter giving a greater surface area in contact with the aqueous phase. The inclusion of surfactant has been previously reported to decrease liposome size in comparison to conventional liposomes. A study formulating liposomes with Phospholipon® 90 G and both Tween 80 and Span 80 reported a size reduction from 207 nm to 139 nm following inclusion of the surfactants [32].

A liposome preparation which is homogenous in size is important as final liposome size will partly determine the level of tissue distribution *in-vivo* in addition to influencing drug release kinetics. A polydispersity of up to 0.3 is considered homogenous [53, 32, 54]. As the loading of surfactant increased, the polydispersity of the liposomal formulation decreased, non-significantly from 0.33 to 0.27 and significantly ( $P < 0.$ ) 0.32 to 0.22 for 'empty'

liposomes (Figure 1a) and those loaded with EGCG respectively (Figure 1b). Therefore, the inclusion of Tween 20 within the liposome formulation appeared to improve homogeneity.

The magnitude of the zeta potential ( $\zeta$ ) indicates the degree of electrostatic repulsion between adjacent, similarly charged particles in a dispersion. Thus, it is a fundamental parameter thought to affect stability of liposomal formulations. All formulated liposomes demonstrated a near neutral charge (Table 1). A neutral liposomal surface charge is important to avoid skin irritation [55] however, this may subsequently lead to particle flocculation due to attractive forces between liposomes causing them to cluster [56].

[Table 1 near here]

In liposomes formulated with EGCG, as Tween 20 loading increased, a statistical significant decrease in EGCG entrapment was observed, ( $P \leq 0.0001$ ), from  $80.0 \pm 3.0$  % no surfactant to  $4.3 \pm 3.0$  % with a 10 % w/w loading of surfactant (Figure 2). This decrease in EGCG loading may be related to the difference in the molecular weight of EGCG and Tween 20. Tween 20, with larger molecular weight of 1227.54 g/mol compared to that of EGCG (386.65 g/mol), may be assumed to be better poised to displace EGCG from the bilayer. Further, the hydrophobic tail of Tween 20 would have a high affinity to the chains in PC therefore displacing EGCG from the bilayer [57-59]. Furthermore, Tween 20 is known to enhance the solubility of drugs and therefore, as not all would be entrapped within the bilayer, this may allow increased EGCG solubilisation within the liposomal rehydration media [60]. It is also possible that the coexistence of vesicles and mixed micelles at high surfactant concentrations [61] may have reduced the compound entrapment in mixed micelles.

[Figure 2 near here]

1  
2  
3 325 The degree of deformability of each formulation was determined by extrusion through  
4  
5 326 a polycarbonate filter with a pore size of 50 nm. The mean particle size and the polydispersity  
6  
7 327 index of liposomes was quantified before and after filtration to assess liposome ability to  
8  
9 328 regain size after having being forced through a pore size smaller than their original diameter.  
10  
11 329 The DI is defined as the degree the liposomes deformed; the greater the degree of  
12  
13 330 deformation the less elastic the liposomes are as they were unable to regain their previous  
14  
15 331 larger size. The DI following extrusion decreased with statistical significance ( $P \leq 0.0001$ ) as  
16  
17 332 surfactant loading increased in 'empty' liposomes, from  $70.8 \pm 6.5$  to  $25.6 \pm 2.9$  % for  
18  
19 333 liposomes formulated with no surfactant compared with  $25.6 \pm 2.93$  for liposomes formulated  
20  
21 334 with 10 % w/w Tween 20 respectively. EGCG liposomes formulated with Tween 20  
22  
23 335 demonstrated a statistically significant decrease ( $P \leq 0.0001$ ) in DI from  $73.66 \pm 8.14$  for  
24  
25 336 liposomes formulated with no surfactant compared with  $37.06 \pm 7.41$  for liposomes  
26  
27 337 formulated with 10 % w/w Tween 20 (Figure 3). These observations imply the liposomes  
28  
29 338 were displaying elastic properties as they could deform in order to pass through an opening  
30  
31 339 smaller than its own diameter whilst, to a certain degree regaining its size. Additionally, the  
32  
33 340 presence of EGCG in the liposome formulation did not appear to affect the DI compared with  
34  
35 341 liposomes formulated without. A study formulating liposomes with Phospholipon® 90 G and  
36  
37 342 both Tween 80 and Span 80 saw a size reduction observed surfactant to decrease the DI from  
38  
39 343  $51.4 \pm 3.6$  to  $17.3 \pm 5.2$  [32].  
40  
41  
42  
43  
44

45 344 [Figure 3 near here]  
46  
47

48 345 Liposomes formulated with surfactant can deform as the surfactant has a propensity  
49  
50 346 for highly curved structures (e.g. micelles and liposomes), thus diminishing the energy  
51  
52 347 required for particle deformation. The surfactant is able to diminish the energy required for  
53  
54 348 particle deformation and accommodate particle shape changes of the liposomes under stress  
55  
56  
57  
58  
59  
60

[62]. These surfactants may have interacted with the PC with strong affinity but in reversible mode. The reversible binding mode might have provided the deformability upon physical stress [38].

For liposomes to deform, a source of energy is required [63-65]. In our systems, 'energy' was supplied to this system in the form of pressure as a result of the action of the syringe driver. The larger the concentration of surfactant included within the formulation, the greater the energy the liposome as a whole is able to retain [65]. It is postulated that this energy is used to reorientate the lipid bilayer structure, and since all systems tend toward the lowest state of free energy, the energy stored in this structure will be expelled once the liposome has passed through the pore and there is no longer any pressure forcing the bilayer to remain in an 'unnatural state' [35, 36, 66]. This energy can then be expended into reforming the liposome. Some energy will be lost during passage as heat or non-plastic deformation, therefore it was not possible to attain a DI of 0 %.

The energy used to alter the bilayer of a liposome containing no surfactant does not benefit from the extra 'storage space' of a surfactant, thus energy may be expended to rupture the membrane causing liposome size to decrease [65]. Despite the potential for excess energy in liposomes formulated with Tween 20, liposomes were not able to fully regain their pre-extrusion size. Some energy will always be lost in the friction of the particles moving through the pores as heat [67]. An increase in surfactant loading may bring the liposomes closer to 100% reformation [65]. Further, liposomes unable to fit through the pores or lipid aggregates from ruptured liposomes may cause blockages. This may lead to an increase in pressure in the vessel causing more turbulence leading to the rupture and non-uniform reformation of liposomes. Additionally, *in-vivo*, liposomes would be expected to move across the skin following an osmotic transepidermal gradient as has been reported in many similar studies

concerning the dermal and transdermal delivery of drug [64, 39, 65, 32]. Such lipid carriers are miscible with the epidermal lipids present within the barrier of the stratum corneum thus would be able to penetrate into deeper layers of the skin [68-70]. Furthermore, the skin is warmer than room temp (35 °C compared to 20 °C). Temperature governs the energy term of enthalpy therefore the liposomes would have more energy to be even more flexible and cross the stratum corneum. M.

### 3.2 Differential scanning calorimetry investigations of EGCG and EGCG lipid blends

Differential scanning calorimetry (DSC) has been widely used in understanding the thermal characteristics of materials where an insight into a range of thermal properties including melting temperatures, phase transitions and heat capacity changes can be obtained. It has been observed that drugs with melting point of < 200 °C are better poised to cross the SC [71, 24], therefore observing the effect of formulation parameters on the melting point would aid formulation development. The glass transition temperature ( $T_g$ ) of EGCG was identified at 220 °C (peak c) and the melting point ( $T_m$ ) of EGCG was at 245 °C (peak d) (Figure 4) and concurred with those reported by Cho et al (2008) where the  $T_m$  of GCG (an epimer of EGCG) was at 223 °C, the  $T_g$  of EGCG was at 235 °C and the  $T_m$  of EGCG was at 246 °C. Cho et al also observed a peak at 97 °C and determined it to be the conversion temperature of EGCG into GCG. Therefore, the first two troughs (peak a and b) observed in the scan may be representative of the epimer GCG [72].

[Figure 4 near here]

The DSC of the lipid (PC and cholesterol) and Tween 20 blend observed the  $T_m$  of this mixture to be 172 °C (Figure 5A). Upon addition of EGCG to this mixture, the melting point shifted to 191 °C (Figure 5B), illustrating that the surfactant loaded liposomes could decrease the  $T_m$  of EGCG thus potentially improving partitioning across the skin [73].

[Figure 5 near here]

### 3.3 EGCG release studies from liposomal formulations

The release of EGCG from solution and liposomal formulations was studied over a 24-hour period (Figure 6). Liposomes appeared to retard the release of EGCG in comparison to release across the membrane from EGCG in solution. Furthermore, with increasing the loading of Tween 20 within liposomal formulations (0 to 10 % w/w), EGCG release increased from  $13.65 \pm 1.12$  % at 24 hours for 0 % w/w Tween 20, to  $94.37 \pm 4.90$  % at 24 hours for 10 % w/w Tween 20. The cumulative percentage released after 24 hours was significant between the solution and liposomes loaded with 0%, 2%, and 6% w/w of Tween 20 ( $P \leq 0.0001$ ). The inclusion of surfactant enables an increase in drug solubility of poorly soluble compounds thus explaining the increase in drug release at higher loadings of surfactant. Such properties are already exploited to improve the oral delivery release profiles of poorly soluble compounds in self-emulsifying drug delivery systems with four drug products [74, 75], Sandimmune® and Sandimmun Neoral® (cyclosporin A), Norvir® (ritonavir), and Fortovase® (saquinavir) on the pharmaceutical market [74]. It is worth noting that as surfactant loading increased, EGCG entrapment decreased thus a lower concentration gradient would be observed. This did not appear to retard EGCG release.

[Figure 6 near here]

An increased rate of release was observed from the EGCG solution compared with liposome formulations over the 24 hours observed (Table 2). Further, as the loading of surfactant increased, the rate of EGCG release increased (from  $0.034 \pm 0.013$  to  $0.993 \pm 1.013$  for liposomes loaded with 0 % and 10 % of Tween 20 respectively based on the Korsmeyer-Peppas model). Thus, surfactant appears to increase drug release, particularly at 10 % w/w where the rate was 10 fold greater than that at 6% w/w. The surfactant would

421 increase drug solubility thus explaining why an increase in drug release is observed at higher  
422 loadings of surfactant. The inclusion of surfactant destabilizes the vesicle bilayers by  
423 reducing the amount of work required to expand the interface allowing the liposome to  
424 become more flexible [40, 38, 39] and move through the membrane. Additionally, it has been  
425 suggested that the mechanism of the *in-vitro* release seems to be the formation of transient  
426 pores in the lipid bilayer, through which drugs are released to the extra-liposomal medium  
427 (Wang, Wang et al. 2016).

428 [Table 2 near here]

429 Based on the values of the determination coefficient ( $R^2$ ), as well as AIC values  
430 (Akaike Information Criterion), the model that best describes EGCG release from all  
431 liposomal formulations is Korsmeyer-Peppas model (highest  $R^2$  and lowest AIC). The  
432 diffusion release exponent value revealed a range of release mechanisms for each  
433 formulation. Liposomes formulated with 0%, 6 % and 10% w/w Tween 20 had an exponent  
434 value of  $0.839 \pm 0.072$ ,  $0.836 \pm 0.116$  and  $0.722 \pm 0.247$  respectively indicating the release is  
435 a complex mixture of the diffusion (flux due to molecular diffusion and the concentration  
436 gradient) and erosion controlled drug release or class-II kinetics (diffusion not based on  
437 concentration gradient) processes and often termed anomalous transport [76]. Liposomes  
438 formulated with 2 % w/w Tween 20 observed an exponent value of  $0.913 \pm 0.186$  indicative  
439 of erosion controlled drug release or class-II kinetics [48].

#### 440 **3.4 Stability of EGCG loaded deformable liposomes**

441 The impact of long-term storage of EGCG-loaded liposomes formulated with 2 %  
442 w/w Tween 20 was assessed during storage in stability cabinets maintained at  $25 \pm 2$  °C  
443 (Firlabo, France) at a humidity of  $60 \% \pm 5$  %. Liposomes formulated with 2% w/w Tween  
444 were selected in this study as it had the highest EGCG entrapment compared with the higher

loadings of surfactant thus will be taken forward for cell uptake studies. The impact of this storage on size (Figure 7) and encapsulation efficiency (Figure 8) was assessed. EGCG loaded liposomes formulated with and without surfactant maintained a consistent size over time (Figure 7) with no statistically significant difference in size during the storage period. Previous reports have highlighted that aggregation is common upon liposomal formulation storage, and results in vesicle size growth [77] particularly with neutral liposomes [56]. However, the inclusion of Tween 20 into the deformable liposomes may have prevented this phenomenon and may be a result of surfactant destabilising the lipid bilayer and reducing the energy required to expand the interface, thus allowing maintenance of smaller structures. It appears the inclusion of surfactant prevents this phenomenon which correlates with similar studies [78].

[Figure 7 and 8 near here]

Furthermore, encapsulation efficiency appears to decrease non-significantly from  $43.02 \pm 6.82 \%$  to  $42.29 \pm 11.63 \%$ ,  $38.76 \pm 9.08 \%$ ,  $30.38 \pm 11.18 \%$  to  $30.33 \pm 6.42 \%$ , for liposomes formulated with 2 % w/w Tween 20 (Figure 8). This suggests drug leaching is independent of surfactant loading. However, Tween 20 is able to increase compound solubility, therefore, as not all would be entrapped within the bilayer, this may allow EGCG to solubilise within the liposomal media [60]. Therefore, as the loading of Tween 20 increased, this would increase the amount of free Tween 20 resulting in more EGCG being able to solubilise in the liposome media.

### 3.5 Cellular toxicity of liposomal formulation towards HDFa and HaCat cells

1  
2  
3 467 Whilst topical formulations are applied directly into the skin, various connective layers  
4  
5 468 making up the skin are important for drug delivery. The skin primarily consists of the  
6  
7 469 epidermis, dermis and subcutaneous layers and each layer has a unique combination of cells,  
8  
9 470 connective tissue, components and functions. Skin cancers develop in the upper layers of the  
10  
11 471 skin spanning the dermal and epidermal layer, and any formulation system should consider  
12  
13 472 the impact of formulation systems on these tissue layers for the delivery of drugs.  
14  
15

16  
17 473 In order to assess cellular toxicity of EGCG to these cells, we adopted two *in-vitro* cell  
18  
19 474 culture systems, namely human keratinocyte and human fibroblast cells. To determine the  
20  
21 475 cellular viability cytotoxicity of EGCG towards HDFa and HaCat cells, an XTT assay was  
22  
23 476 performed to measure cell death after exposure of cells to different concentrations of drug for  
24  
25 477 24 hours (Figure 9).  
26

27  
28 478 [Figure 9 near here]  
29  
30

31  
32 479 As the concentration of EGCG was increased from 0.1 to 100  $\mu$ M, HDFa cell viability  
33  
34 480 decreased (Figure 9A) with statistical significance ( $P \leq 0.0001$ ). This may be due to toxicity  
35  
36 481 or death of damaged cells in which EGCG induced apoptosis [79, 80]. Whilst limited data  
37  
38 482 exists on the cytotoxicity of EGCG towards dermal tissues, a study observing growth  
39  
40 483 inhibition in multiple cell lines, observed that EGCG at 40  $\mu$ M had little or no inhibitory  
41  
42 484 effect on the growth of WI38 cells, normal human fibroblast cells [81]. Cell viability was  
43  
44 485 maintained across the concentration range of 0.1–100  $\mu$ M on HaCat cells (Figure 9B). No  
45  
46 486 statistically significant difference was observed in cell viability ( $P \geq 0.05$ ). Furthermore,  
47  
48 487 EGCG has been reported to impart protective effects in HaCat cells exposed to external  
49  
50 488 stressors including UVA and UVB radiation [82, 83]. Whilst some of our formulations  
51  
52 489 exceeded this concentration of EGCG as a whole, the retarded release profile of the  
53  
54  
55  
56  
57  
58  
59  
60

liposomes would be expected to result in an overall lower temporal concentration profile exposure to these cells, significantly below 100  $\mu$ M.

### 3.6 Cellular liposomal uptake assay into HDFa and HaCat cells

A primary goal for our studies was to demonstrate uptake of deformable liposomes loaded with EGCG into a cell culture skin model. EGCG loaded liposomes were incubated with both HaCat (Figure 10) and HDFa (Figure 11) cells to assess the cellular uptake of these formulations. Liposomes formulated with 2% w/w Tween 20 were selected, a result of the highest EGCG entrapment compared with the other surfactant loadings. DilC labelled liposomes loaded with EGCG incubated for 2-hours with both HaCat and HDFa cells seeded onto collagen-coated coverslips and the cellular localisation of these liposomes was determined using confocal microscopy. Following a 2-hour incubation with the cells, intracellular localisation of labelled liposomes were clearly evident, confirming the successful uptake into both HaCat and HDFa cells.

[Figure 10 and 11 near here]

Extraneous particle cell uptake is dependent upon influences such as particle size, charge, affinity etc. [84-86]. There are four proposed methods of liposome uptake into cells: stable adsorption, endocytosis, fusion of the lipid bilayer with the cell plasma membrane and lipid transfer [43, 87]. It is unclear which of these occurred in this study, however, these methods of uptake are not mutually exclusive and any combination may occur in a given experimental circumstance [43]. The interaction of nanoparticles with cell membrane seems to be most affected by particle surface charge. The cell membrane surface is dominated by negatively charged sulphated proteoglycans molecules (vital in cellular proliferation and migration) [88, 89]. These molecules are associated with glycosaminoglycan side chains (heparan, dermatan, keratan or chondrotine sulfates) which are anionic, and interaction

between proteoglycans and liposomes, if positively charged, tend to be largely ionic [90]. The liposomes applied to the cells in this study had a  $\zeta$  of  $3.67 \pm 0.91$  suggesting an ionic interaction may have occurred. A study applying cationic liposomes formulated with the cationic lipids Lipofectin, Tfx-50, and Lipofectamine in oligonucleotide delivery to HaCat cells observed liposome uptake within 24 hours [91]. Furthermore, research developing chemotherapy against malignant melanoma using mouse B16 melanoma cells as well as Normal Human Dermal Fibroblasts observed a greater uptake of cationic liposomes by cells in the injection site compared with neutral liposomes due to the electrostatic interaction with the negative-charged phospholipid membrane of cells [92].

It should be noted that the confocal microscopy studies demonstrated the possibility of the delivery of deformable liposomes to relevant dermal tissues using *in-vitro* cell culture techniques. However, the application of such formulations could also be assessed using *ex-vivo* human or animal dermal tissues. The ultimate aim of this delivery system was to improve dermal cell uptake and delivery a controlled release of active agent, thus from a regulatory perspective, pharmacokinetic data is not required as drug is not intended to reach the blood stream [93].

In order to ascertain the extent of carrier and drug permeation a skin strip test may be appropriate [70]. This involves the use of an adhesive tape to strip the skin layer by layer and quantifying lipid and drug on each layer[94]. Further, whilst the most appropriate animal model for human skin is the porcine skin tissue, sample-to-sample variability in addition to differences in the lipid dermal matrices often results in an altered permeability profile limiting the wider human translational goals [95-97].

#### 4. Conclusion

1  
2  
3 537 Skin cancer is emerging as an increasing public health problem particularly in  
4  
5 538 developed countries. Current treatments include surgery to remove the tumour as well as  
6  
7 539 topical formulations. Such treatments may not be suitable for all patients as they are  
8  
9 540 associated with an unpleasant aesthetic profile as well as side effects. A nanoparticle delivery  
10  
11 541 system such as deformable liposomes applied topically for the direct dermal delivery of  
12  
13 542 compounds would be valuable in carrying compounds across the stratum corneum at a  
14  
15 543 controlled rate whilst limiting side effects. The use of naturally occurring compounds such as  
16  
17 544 EGCG have been found to be successful as chemopreventative and chemoprotective agents.  
18  
19 545 However, formulation of such compounds has been limited in success due to a limited  
20  
21 546 bioavailability of promising agents and inefficient delivery systems. We developed a novel  
22  
23 547 deformable liposome formulation loaded with EGCG and systemically investigated the  
24  
25 548 loading, uptake and *in-vitro* release of EGCG from these nanoparticles. This study has found  
26  
27 549 deformable liposomes could be valuable in enhancing the bioavailability of these compounds  
28  
29 550 as well as offering controlled release of the compound [13, 98]. We have demonstrated that  
30  
31 551 as the amount of Tween 20 in the liposomal bilayer is increased, liposome size decreased and  
32  
33 552 elasticity increased. As the loading of Tween 20 in the liposome was increased the EGCG  
34  
35 553 encapsulation decreased. This may have been due to Tween 20 competing for space within  
36  
37 554 the bilayer or due to Tween 20 increasing the solubilisation capacity of EGCG. Additionally  
38  
39 555 EGCG release from liposomes found that the liposomes were able to modify the release of  
40  
41 556 drug with complete release observed within 24 hours. Further, our studies demonstrated these  
42  
43 557 liposomes were capable of uptake into epidermal keratinocytes and dermal fibroblasts within  
44  
45 558 2 hours. This present study demonstrates liposomes formulated with Tween 20 are useful in  
46  
47 559 enhancing drug penetration into dermal cells and in the development of a controlled release  
48  
49 560 formulation crucial in improving patient compliance thus skin cancer treatment outcomes.  
50  
51  
52  
53  
54  
55

56 **Disclosure of interest**  
57  
58  
59  
60

The authors report no conflict of interest.

## References

1. Lomas A, Leonardi-Bee J, Bath-Hextall F. A systematic review of worldwide incidence of nonmelanoma skin cancer. *The British journal of dermatology*. 2012;166(5):1069-80. doi:10.1111/j.1365-2133.2012.10830.x.
2. World Health Organisation. Ultraviolet radiation (UV): Skin cancers. 2017. <http://www.who.int/uv/faq/skincancer/en/index1.html>. Accessed 20/11/2017 2017.
3. Diepgen TL, Mahler V. The epidemiology of skin cancer. *The British journal of dermatology*. 2002;146 Suppl 61(s61):1-6.
4. Donaldson MR, Coldiron BM, editors. No end in sight: the skin cancer epidemic continues. *Seminars in cutaneous medicine and surgery*; 2011: Frontline Medical Communications.
5. American Cancer Society. Cancer Facts and Figures. 2017. <http://www.cancer.org/acs/groups/content/@editorial/documents/document/acspc-048738.pdf>. Accessed 10/01/2017 2017.
6. Ali SM, Brodell RT, Balkrishnan R, Feldman SR. Poor adherence to treatments: A fundamental principle of dermatology. *Archives of dermatology*. 2007;143(7):912-5. doi:10.1001/archderm.143.7.912.
7. Felicio L, Ferreira J, Kurachi C, Bentley M, Tedesco A, Bagnato V. Long-term follow-up of topical 5-aminolaevulinic acid photodynamic therapy diode laser single session for non-melanoma skin cancer. *Photodiagnosis and photodynamic therapy*. 2009;6:207-13.
8. Kaplan B, Moy RL. Effect of perilesional injections of PEG-interleukin-2 on basal cell carcinoma. *Dermatol Surg*. 2000;26(11):1037-40.

- 585 9. Neville JA, Welch E, Leffell DJ. Management of nonmelanoma skin cancer in 2007. *Nat*  
586 *Clin Prac Oncol*. 2007;4(8):462-9.
- 587 10. Bansal T, Jaggi M, Khar R, Talegaonkar S. Emerging significance of flavonoids as P-  
588 glycoprotein inhibitors in cancer chemotherapy. *Journal of Pharmacy & Pharmaceutical*  
589 *Sciences*. 2009;12(1):46-78.
- 590 11. Kanadaswami C, Lee L-T, Lee P-PH, Hwang J-J, Ke F-C, Huang Y-T et al. The  
591 antitumor activities of flavonoids. *In Vivo*. 2005;19(5):895-909.
- 592 12. Carey MP, Burish TG. Etiology and treatment of the psychological side effects associated  
593 with cancer chemotherapy: A critical review and discussion. *Psychological bulletin*.  
594 1988;104(3):307.
- 595 13. Siddiqui IA, Adhami VM, Bharali DJ, Hafeez BB, Asim M, Khwaja SI et al. Introducing  
596 Nanochemoprevention as a Novel Approach for Cancer Control: Proof of Principle with  
597 Green Tea Polyphenol Epigallocatechin-3-Gallate. *Cancer research*. 2009;69(5):1712-6.  
598 doi:10.1158/0008-5472.can-08-3978.
- 599 14. Hwang J-T, Ha J, Park I-J, Lee S-K, Baik HW, Kim YM et al. Apoptotic effect of EGCG  
600 in HT-29 colon cancer cells via AMPK signal pathway. *Cancer letters*. 2007;247(1):115-21.  
601 doi:<http://dx.doi.org/10.1016/j.canlet.2006.03.030>.
- 602 15. Singh BN, Shankar S, Srivastava RK. Green tea catechin, epigallocatechin-3-gallate  
603 (EGCG): Mechanisms, perspectives and clinical applications. *Biochemical pharmacology*.  
604 2011;82(12):1807-21. doi:<http://dx.doi.org/10.1016/j.bcp.2011.07.093>.
- 605 16. Casey SC, Amedei A, Aquilano K, Azmi AS, Benencia F, Bhakta D et al. Cancer  
606 prevention and therapy through the modulation of the tumor microenvironment. *Seminars in*  
607 *cancer biology*. 2015. doi:10.1016/j.semcancer.2015.02.007.

17. Gupta S, Hastak K, Afaq F, Ahmad N, Mukhtar H. Essential role of caspases in epigallocatechin-3-gallate-mediated inhibition of nuclear factor kappa B and induction of apoptosis. *Oncogene*. 2004;23(14):2507-22. doi:10.1038/sj.onc.1207353.
18. Singh T, Vaid M, Katiyar N, Sharma S, Katiyar SK. Berberine, an isoquinoline alkaloid, inhibits melanoma cancer cell migration by reducing the expressions of cyclooxygenase-2, prostaglandin E(2) and prostaglandin E(2) receptors. *Carcinogenesis*. 2011;32(1):86-92. doi:10.1093/carcin/bgq215.
19. Thawonsuwan J, Kiron V, Satoh S, Panigrahi A, Verlhac V. Epigallocatechin-3-gallate (EGCG) affects the antioxidant and immune defense of the rainbow trout, *Oncorhynchus mykiss*. *Fish physiology and biochemistry*. 2010;36(3):687-97. doi:10.1007/s10695-009-9344-4.
20. Sigler K, Ruch RJ. Enhancement of gap junctional intercellular communication in tumor promoter-treated cells by components of green tea. *Cancer letters*. 1993;69(1):15-9.
21. Basnet P, Hussain H, Tho I, Skalko-Basnet N. Liposomal delivery system enhances anti-inflammatory properties of curcumin. *J Pharm Sci*. 2012;101(2):598-609. doi:10.1002/jps.22785.
22. Wang Y, Wang S, Firempong CK, Zhang H, Wang M, Zhang Y et al. Enhanced Solubility and Bioavailability of Naringenin via Liposomal Nanoformulation: Preparation and In Vitro and In Vivo Evaluations. *Aaps Pharmscitech*. 2016. doi:10.1208/s12249-016-0537-8.
23. Zhao Y-Z, Lu C-T, Zhang Y, Xiao J, Zhao Y-P, Tian J-L et al. Selection of high efficient transdermal lipid vesicle for curcumin skin delivery. *Int J Pharmaceut*. 2013;454(1):302-9.
24. Alexander A, Dwivedi S, Giri TK, Saraf S, Saraf S, Tripathi DK. Approaches for breaking the barriers of drug permeation through transdermal drug delivery. *J Control Release*. 2012;164(1):26-40.

25. Lopez RF, Seto JE, Blankschtein D, Langer R. Enhancing the transdermal delivery of rigid nanoparticles using the simultaneous application of ultrasound and sodium lauryl sulfate. *Biomaterials*. 2011;32(3):933-41. doi:10.1016/j.biomaterials.2010.09.060.
26. Tsai MJ, Huang YB, Fang JW, Fu YS, Wu PC. Preparation and Characterization of Naringenin-Loaded Elastic Liposomes for Topical Application. *PloS one*. 2015;10(7):e0131026. doi:10.1371/journal.pone.0131026.
27. Alexander A, Dwivedi S, Ajazuddin, Giri TK, Saraf S, Saraf S et al. Approaches for breaking the barriers of drug permeation through transdermal drug delivery. *J Control Release*. 2012;164(1):26-40. doi:DOI 10.1016/j.jconrel.2012.09.017.
28. Bouwstra JA, Honeywell-Nguyen PL. Skin structure and mode of action of vesicles. *Adv Drug Deliv Rev*. 2002;54 Suppl 1:S41-55.
29. du Plessis J, Weiner N, Müller D. The influence of in vivo treatment of skin with liposomes on the topical absorption of a hydrophilic and a hydrophobic drug in vitro. *Int J Pharmaceut*. 1994;103(2):R1-R5.
30. Park S-I, Lee E-O, Yang H-M, Park CW, Kim J-D. Polymer-hybridized liposomes of poly (amino acid) derivatives as transepidermal carriers. *Colloids and Surfaces B: Biointerfaces*. 2013;110:333-8.
31. Cevc G, Gebauer D, Stieber J, Schätzlein A, Blume G. Ultraflexible vesicles, Transfersomes, have an extremely low pore penetration resistance and transport therapeutic amounts of insulin across the intact mammalian skin. *Biochimica et Biophysica Acta (BBA) - Biomembranes*. 1998;1368(2):201-15. doi:[http://dx.doi.org/10.1016/S0005-2736\(97\)00177-6](http://dx.doi.org/10.1016/S0005-2736(97)00177-6).
32. Goindi S, Kumar G, Kumar N, Kaur A. Development of novel elastic vesicle-based topical formulation of cetirizine dihydrochloride for treatment of atopic dermatitis. *Aaps Pharmscitech*. 2013;14(4):1284-93. doi:10.1208/s12249-013-0017-3.

33. El MGMM, C. WA, W. BB. Skin delivery of 5-fluorouracil from ultradeformable and standard liposomes in-vitro. *J Pharm Pharmacol.* 2001;53(8):1069-77. doi:doi:10.1211/0022357011776450.
34. Cevc GS, A.; Gebauer, D.; Blume, G. Ultra-high efficiency of drug and peptide transfer through the intact skin by means of novel drug-carriers, Transfersomes. In: Bain KRH, J.; James, W.J.; Water, K.A., editor. *Prediction of Percutaneous Penetration*. Cardiff: STS Publishing; 1993. p. 226-34.
35. Cevc G, Schätzlein A, Gebauer D, Blume G. Ultra-high efficiency of drugs and peptide transfer through the intact skin by means of novel drug carriers, transfersomes. STS Publishing; 1993.
36. Cevc G. Material transport across permeability barriers by means of lipid vesicles. *Handbook of biological physics*. 1995;1:465-90.
37. Romero EL, Morilla MJ. Highly deformable and highly fluid vesicles as potential drug delivery systems: theoretical and practical considerations. *Int J Nanomedicine*. 2013;8:3171-86. doi:10.2147/ijn.s33048.
38. Oh YK, Kim MY, Shin JY, Kim TW, Yun MO, Yang SJ et al. Skin permeation of retinol in Tween 20-based deformable liposomes: in-vitro evaluation in human skin and keratinocyte models. *J Pharm Pharmacol*. 2006;58(2):161-6. doi:10.1211/jpp.58.2.0002.
39. Cevc G. Transfersomes, liposomes and other lipid suspensions on the skin: permeation enhancement, vesicle penetration, and transdermal drug delivery. *Crit Rev Ther Drug Carrier Syst*. 1996;13(3-4):257-388.
40. Ita KB, Du Preez J, Lane ME, Hadgraft J, du Plessis J. Dermal delivery of selected hydrophilic drugs from elastic liposomes: effect of phospholipid formulation and surfactants. *J Pharm Pharmacol*. 2007;59(9):1215-22. doi:10.1211/jpp.59.9.0005.

41. Bangham AD, Standish MM, Watkins JC. Diffusion of univalent ions across the lamellae of swollen phospholipids. *Journal of molecular biology*. 1965;13(1):238-52.
42. Hiruta Y, Hattori Y, Kawano K, Obata Y, Maitani Y. Novel ultra-deformable vesicles entrapped with bleomycin and enhanced to penetrate rat skin. *J Control Release*. 2006;113(2):146-54. doi:<http://dx.doi.org/10.1016/j.jconrel.2006.04.016>.
43. Pagano RE, Weinstein JN. Interactions of liposomes with mammalian cells. *Annual review of biophysics and bioengineering*. 1978;7(1):435-68.
44. Ali MH, Moghaddam B, Kirby DJ, Mohammed AR, Perrie Y. The role of lipid geometry in designing liposomes for the solubilisation of poorly water soluble drugs. *Int J Pharmaceut*. 2013;453(1):225-32. doi:DOI 10.1016/j.ijpharm.2012.06.056.
45. Lasic DD, Barenholz Y. *Handbook of nonmedical applications of liposomes: Theory and basic sciences*. CRC Press; 1996.
46. Song Y-K, Kim C-K. Topical delivery of low-molecular-weight heparin with surface-charged flexible liposomes. *Biomaterials*. 2006;27(2):271-80. doi:<http://dx.doi.org/10.1016/j.biomaterials.2005.05.097>.
47. Bradfield A, Penney M. 456. The catechins of green tea. Part II. *Journal of the Chemical Society (Resumed)*. 1948:2249-54.
48. Korsmeyer RW, Gurny R, Doelker E, Buri P, Peppas NA. Mechanisms of solute release from porous hydrophilic polymers. *Int J Pharmaceut*. 1983;15(1):25-35. doi:[http://dx.doi.org/10.1016/0378-5173\(83\)90064-9](http://dx.doi.org/10.1016/0378-5173(83)90064-9).
49. Scudiero DA, Shoemaker RH, Paull KD, Monks A, Tierney S, Nofziger TH et al. Evaluation of a soluble tetrazolium/formazan assay for cell growth and drug sensitivity in culture using human and other tumor cell lines. *Cancer research*. 1988;48(17):4827-33.

50. Yang CS, Maliakal P, Meng X. Inhibition of carcinogenesis by tea. Annual review of pharmacology and toxicology. 2002;42:25-54. doi:10.1146/annurev.pharmtox.42.082101.154309.
51. McLoughlin P, Roengvoraphoj M, Gissel C, Hescheler J, Certa U, Sachinidis A. Transcriptional responses to epigallocatechin-3 gallate in HT 29 colon carcinoma spheroids. Genes to cells : devoted to molecular & cellular mechanisms. 2004;9(7):661-9. doi:10.1111/j.1356-9597.2004.00754.x.
52. El Zaafarany GM, Awad GA, Holayel SM, Mortada ND. Role of edge activators and surface charge in developing ultradeformable vesicles with enhanced skin delivery. Int J Pharmaceut. 2010;397(1):164-72.
53. Chen Y, Wu Q, Zhang Z, Yuan L, Liu X, Zhou L. Preparation of curcumin-loaded liposomes and evaluation of their skin permeation and pharmacodynamics. Molecules. 2012;17(5):5972-87. doi:10.3390/molecules17055972.
54. Kang SN, Hong S-S, Kim S-Y, Oh H, Lee M-K, Lim S-J. Enhancement of liposomal stability and cellular drug uptake by incorporating tributyrin into celecoxib-loaded liposomes. Asian Journal of Pharmaceutical Sciences. 2013;8(2):128-33. doi:<http://dx.doi.org/10.1016/j.ajps.2013.07.016>.
55. Prausnitz MR, Langer R. Transdermal drug delivery. Nat Biotech. 2008;26(11):1261-8.
56. Weiner N, Egbaria K, Ramachandran C. Topical Delivery of Liposomally Encapsulated Interferon Evaluated by In Vitro Diffusion Studies and in a Cutaneous Herpes Guinea Pig Model. In: Braun-Falco O, Korting HC, Maibach HI, editors. Liposome Dermatics: Griesbach Conference. Berlin, Heidelberg: Springer Berlin Heidelberg; 1992. p. 242-50.
57. El Maghraby GMM, Williams AC, Barry BW. Oestradiol skin delivery from ultradeformable liposomes: refinement of surfactant concentration. Int J Pharmaceut. 2000;196(1):63-74. doi:[http://dx.doi.org/10.1016/S0378-5173\(99\)00441-X](http://dx.doi.org/10.1016/S0378-5173(99)00441-X).

58. Levy MY, Benita S, Baszkin A. Interactions of a non-ionic surfactant with mixed phospholipid—oleic acid monolayers. Studies under dynamic conditions. *Colloid Surface*. 1991;59:225-41. doi:[http://dx.doi.org/10.1016/0166-6622\(91\)80249-N](http://dx.doi.org/10.1016/0166-6622(91)80249-N).
59. Casas M, Baszkin A. Interactions of a non-ionic surfactant with mixed phospholipid—oleic acid monolayers. Surface potential and surface pressure studies at constant area. *Colloid Surface*. 1992;63(3):301-9. doi:[http://dx.doi.org/10.1016/0166-6622\(92\)80252-W](http://dx.doi.org/10.1016/0166-6622(92)80252-W).
60. Almog S, Kushnir T, Nir S, Lichtenberg D. Kinetic and structural aspects of reconstitution of phosphatidylcholine vesicles by dilution of phosphatidylcholine-sodium cholate mixed micelles. *Biochemistry*. 1986;25(9):2597-605.
61. Almog S, Kushnir T, Nir S, Lichtenberg D. Kinetic and structural aspects of reconstitution of phosphatidylcholine vesicles by dilution of phosphatidylcholine-sodium cholate mixed micelles. *Biochemistry*. 1986;25(9):2597-605.
62. Trotta M, Peira E, Carlotti ME, Gallarate M. Deformable liposomes for dermal administration of methotrexate. *Int J Pharm*. 2004;270(1-2):119-25.
63. Fresta M, Puglisi G. Application of liposomes as potential cutaneous drug delivery systems. In vitro and in vivo investigation with radioactively labelled vesicles. *J Drug Target*. 1996;4(2):95-101. doi:10.3109/10611869609046267.
64. Gompper G, Kroll DM. Driven transport of fluid vesicles through narrow pores. *Physical review E, Statistical physics, plasmas, fluids, and related interdisciplinary topics*. 1995;52(4):4198-208.
65. Trotta M, Peira E, Debernardi F, Gallarate M. Elastic liposomes for skin delivery of dipotassium glycyrrhizinate. *Int J Pharmaceut*. 2002;241(2):319-27. doi:[http://dx.doi.org/10.1016/S0378-5173\(02\)00266-1](http://dx.doi.org/10.1016/S0378-5173(02)00266-1).
66. Chung H, Caffrey M. The curvature elastic-energy function of the lipid-water cubic mesophase. *Nature*. 1994;368(6468):224-6. doi:10.1038/368224a0.

67. Vajjha RS, Das DK, Kulkarni DP. Development of new correlations for convective heat transfer and friction factor in turbulent regime for nanofluids. *International Journal of Heat and Mass Transfer*. 2010;53(21):4607-18. doi:<http://dx.doi.org/10.1016/j.ijheatmasstransfer.2010.06.032>.
68. Kirjavainen M, Urtti A, Jääskeläinen I, Marjukka Suhonen T, Paronen P, Valjakka-Koskela R et al. Interaction of liposomes with human skin in vitro — The influence of lipid composition and structure. *Biochimica et Biophysica Acta (BBA) - Lipids and Lipid Metabolism*. 1996;1304(3):179-89. doi:[http://dx.doi.org/10.1016/S0005-2760\(96\)00126-9](http://dx.doi.org/10.1016/S0005-2760(96)00126-9).
69. El Maghraby GM, Barry BW, Williams AC. Liposomes and skin: From drug delivery to model membranes. *Eur J Pharm Sci*. 2008;34(4–5):203-22. doi:<http://dx.doi.org/10.1016/j.ejps.2008.05.002>.
70. Schäfer-Korting M, Mehnert W, Korting H-C. Lipid nanoparticles for improved topical application of drugs for skin diseases. *Adv Drug Deliver Rev*. 2007;59(6):427-43. doi:<http://dx.doi.org/10.1016/j.addr.2007.04.006>.
71. Guy RH, Hadgraft J. Transdermal drug delivery: a simplified pharmacokinetic approach. *Int J Pharmaceut*. 1985;24(2-3):267-74.
72. Cho HH, Han D-W, Matsumura K, Tsutsumi S, Hyon S-H. The behavior of vascular smooth muscle cells and platelets onto epigallocatechin gallate-releasing poly(l-lactide-co-ε-caprolactone) as stent-coating materials. *Biomaterials*. 2008;29(7):884-93. doi:<http://dx.doi.org/10.1016/j.biomaterials.2007.10.052>.
73. Chu KA, Yalkowsky SH. An interesting relationship between drug absorption and melting point. *Int J Pharm*. 2009;373(1-2):24-40. doi:10.1016/j.ijpharm.2009.01.026.
74. Neslihan Gursoy R, Benita S. Self-emulsifying drug delivery systems (SEDDS) for improved oral delivery of lipophilic drugs. *Biomedicine & Pharmacotherapy*. 2004;58(3):173-82. doi:<https://doi.org/10.1016/j.biopha.2004.02.001>.

- 780 75. Vasconcelos T, Sarmiento B, Costa P. Solid dispersions as strategy to improve oral  
781 bioavailability of poor water soluble drugs. *Drug discovery today*. 2007;12(23):1068-75.  
782 doi:<https://doi.org/10.1016/j.drudis.2007.09.005>.
- 783 76. Peppas NA, Sahlin JJ. A simple equation for the description of solute release. III.  
784 Coupling of diffusion and relaxation. *Int J Pharmaceut*. 1989;57(2):169-72.  
785 doi:[http://dx.doi.org/10.1016/0378-5173\(89\)90306-2](http://dx.doi.org/10.1016/0378-5173(89)90306-2).
- 786 77. Lentz BR, Carpenter TJ, Alford DR. Spontaneous fusion of phosphatidylcholine small  
787 unilamellar vesicles in the fluid phase. *Biochemistry*. 1987;26(17):5389-97.
- 788 78. Seras M, Handjani-Vila R-M, Ollivon M, Lesieur S. Kinetic aspects of the solubilization  
789 of non-ionic monoalkyl amphiphile-cholesterol vesicles by octylglucoside. *Chem Phys*  
790 *Lipids*. 1992;63(1-2):1-14. doi:[http://dx.doi.org/10.1016/0009-3084\(92\)90015-H](http://dx.doi.org/10.1016/0009-3084(92)90015-H).
- 791 79. Bae JY, Choi JS, Choi YJ, Shin SY, Kang SW, Han SJ et al. (-)Epigallocatechin gallate  
792 hampers collagen destruction and collagenase activation in ultraviolet-B-irradiated human  
793 dermal fibroblasts: involvement of mitogen-activated protein kinase. *Food and chemical*  
794 *toxicology : an international journal published for the British Industrial Biological Research*  
795 *Association*. 2008;46(4):1298-307. doi:10.1016/j.fct.2007.09.112.
- 796 80. Tanigawa T, Kanazawa S, Ichibori R, Fujiwara T, Magome T, Shingaki K et al. (+)-  
797 Catechin protects dermal fibroblasts against oxidative stress-induced apoptosis. *BMC*  
798 *complementary and alternative medicine*. 2014;14:133. doi:10.1186/1472-6882-14-133.
- 799 81. Chen ZP, Schell JB, Ho C-T, Chen KY. Green tea epigallocatechin gallate shows a  
800 pronounced growth inhibitory effect on cancerous cells but not on their normal counterparts.  
801 *Cancer letters*. 1998;129(2):173-9. doi:[http://dx.doi.org/10.1016/S0304-3835\(98\)00108-6](http://dx.doi.org/10.1016/S0304-3835(98)00108-6).
- 802 82. Huang C-C, Fang J-Y, Wu W-B, Chiang H-S, Wei Y-J, Hung C-F. Protective effects of  
803 (-)-epicatechin-3-gallate on UVA-induced damage in HaCaT keratinocytes. *Archives of*  
804 *dermatological research*. 2005;296(10):473-81.

- 805 83. Huang C-C, Wu W-B, Fang J-Y, Chiang H-S, Chen S-K, Chen B-H et al. (-)-Epicatechin-  
806 3-gallate, a green tea polyphenol is a potent agent against UVB-induced damage in HaCaT  
807 keratinocytes. *Molecules*. 2007;12(8):1845-58.
- 808 84. Patil S, Sandberg A, Heckert E, Self W, Seal S. Protein adsorption and cellular uptake of  
809 cerium oxide nanoparticles as a function of zeta potential. *Biomaterials*. 2007;28(31):4600-7.  
810 doi:10.1016/j.biomaterials.2007.07.029.
- 811 85. Chen C-C, Tsai T-H, Huang Z-R, Fang J-Y. Effects of lipophilic emulsifiers on the oral  
812 administration of lovastatin from nanostructured lipid carriers: Physicochemical  
813 characterization and pharmacokinetics. *Eur J Pharm Biopharm*. 2010;74(3):474-82.  
814 doi:<https://doi.org/10.1016/j.ejpb.2009.12.008>.
- 815 86. Kyung OY, Grabinski CM, Schrand AM, Murdock RC, Wang W, Gu B et al. Toxicity of  
816 amorphous silica nanoparticles in mouse keratinocytes. *Journal of Nanoparticle Research*.  
817 2009;11(1):15-24.
- 818 87. Martin FJ, MacDonald RC. Lipid vesicle-cell interactions. I. Hemagglutination and  
819 hemolysis. *The Journal of cell biology*. 1976;70(3):494-505.
- 820 88. Merton Bernfield, Martin Götte, Pyong Woo Park, Ofer Reizes, Marilyn L. Fitzgerald,  
821 John Lincecum et al. Functions of Cell Surface Heparan Sulfate Proteoglycans. *Annual*  
822 *Review of Biochemistry*. 1999;68(1):729-77. doi:10.1146/annurev.biochem.68.1.729.
- 823 89. Mislick KA, Baldeschwieler JD. Evidence for the role of proteoglycans in cation-  
824 mediated gene transfer. *Proceedings of the National Academy of Sciences*.  
825 1996;93(22):12349-54.
- 826 90. Panyam J, Labhasetwar V. Biodegradable nanoparticles for drug and gene delivery to  
827 cells and tissue. *Adv Drug Deliv Rev*. 2003;55(3):329-47.
- 828 91. White PJ, Fogarty RD, McKean SC, Venables DJ, Werther GA, Wraight CJ.  
829 Oligonucleotide Uptake in Cultured Keratinocytes: Influence of Confluence, Cationic

- 1  
2  
3 830 Liposomes, and Keratinocyte Cell Type. J Invest Dermatol. 1999;112(5):699-705.  
4  
5 831 doi:<https://doi.org/10.1046/j.1523-1747.1999.00578.x>.  
6  
7 832 92. Ito A, Fujioka M, Yoshida T, Wakamatsu K, Ito S, Yamashita T et al. 4-S-  
8  
9 833 Cysteaminyphenol-loaded magnetite cationic liposomes for combination therapy of  
10  
11 834 hyperthermia with chemotherapy against malignant melanoma. Cancer science.  
12  
13 835 2007;98(3):424-30. doi:10.1111/j.1349-7006.2006.00382.x.  
14  
15 836 93. Products EAftEoM. Note for Guidance on the Investigation of Bioavailability and  
16  
17 837 Bioequivalence. London: European Agency for the Evaluation of Medicinal Products  
18  
19  
20 838 2000 14/12/2000.  
21  
22 839 94. Weigmann H, Lademann J, Meffert H, Schaefer H, Sterry W. Determination of the horny  
23  
24 840 layer profile by tape stripping in combination with optical spectroscopy in the visible range as  
25  
26 841 a prerequisite to quantify percutaneous absorption. Skin Pharmacol Appl Skin Physiol.  
27  
28 842 1999;12(1-2):34-45. doi:10.1159/000029844.  
29  
30 843 95. Schmook FP, Meingassner JG, Billich A. Comparison of human skin or epidermis models  
31  
32 844 with human and animal skin in in-vitro percutaneous absorption. Int J Pharmaceut.  
33  
34 845 2001;215(1-2):51-6.  
35  
36 846 96. Dick IP, Scott RC. Pig ear skin as an in - vitro model for human skin permeability. J  
37  
38 847 Pharm Pharmacol. 1992;44(8):640-5.  
39  
40 848 97. Godin B, Touitou E. Transdermal skin delivery: predictions for humans from in vivo, ex  
41  
42 849 vivo and animal models. Adv Drug Deliver Rev. 2007;59(11):1152-61.  
43  
44 850 98. Nishiyama N. Nanomedicine: Nanocarriers shape up for long life. Nat Nano.  
45  
46 851 2007;2(4):203-4.  
47  
48  
49 852  
50  
51  
52  
53  
54  
55 853  
56  
57  
58  
59  
60

**Table 1:** Zeta potential of liposomal formulations formulated in the absence and presence of up to 10% w/w of Tween 20

Surfactant loading (% w/w)	Zeta potential (mV)	
	'empty'	EGCG loaded
	liposomes	liposomes
0	5.03 ± 1.03	2.41 ± 1.08
2	4.67 ± 1.08	3. 67 ± 0.91
6	3.71 ± 0.90	-0.99 ± 1.01
10	-2.79 ± 0.20	-1.90 ± 0.88

Results are presented as the mean ± standard deviation (n=3)

Table 2: *In-vitro* SA release kinetics models

Kinetic model	Parameter	Tween 20 Loading (% w/w)			
		0	2	6	10
0	$(k_0) \times 10^{-2}$	1.01 ± 0.05	1.18 ± 0.01	2.75 ± 0.05	7.77 ± 0.02
	mg • min <sup>-1</sup>				
	R <sup>2</sup>	0.95 ± 0.02	0.99 ± 0.01	0.93 ± 0.07	0.72 ± 0.30
	AIC	28.59 ± 4.44	18.82 ± 2.96	57.24 ± 14.21	98.21 ± 25.32
1 <sup>st</sup>	$(k_1) \times 10^{-4}$	1.07 ± 0.05	1.27 ± 0.13	3.32 ± 0.58	15.04 ± 3.11
	min <sup>-1</sup>				
	R <sup>2</sup>	0.96 ± 0.02	0.986 ± 0.01	0.96 ± 0.04	0.94 ± 0.06
	AIC	25.68 ± 4.40	18.132 ± 6.83	54.03 ± 6.46	4.56 ± 17.86
Higuchi	k <sub>H</sub>	0.26 ± 0.01	0.294 ± 0.03	0.71 ± 0.09	2.12 ± 0.14
	R <sup>2</sup>	0.83 ± 0.04	0.7513 ± 0.03	0.81 ± 0.05	0.86 ± 0.10
	AIC	47.40 ± 5.92	58.783 ± 4.90	77.32 ± 9.63	99.05 ± 13.13
	k <sub>KP</sub>	0.03 ± 0.01	0.059 ± 0.08	0.09 ± 0.06	0.99 ± 1.01
Korsmeyer-Peppas	N	0.84 ± 0.07	0.913 ± 0.19	0.84 ± 0.12	0.72 ± 0.25
	R <sup>2</sup>	<b>0.99 ± 0.01</b>	<b>0.991 ± 0.01</b>	<b>0.99 ± 0.01</b>	<b>0.96 ± 0.03</b>
	AIC	11.26 ± 3.00	27.163 ± 22.24	49.82 ± 8.49	82.76 ± 9.81

R<sup>2</sup>, coefficient of determination; AIC, Akaike Information Criterion; F is the fraction of drug released at time t; k<sub>0</sub> is the zero-order release constant; k<sub>1</sub> is the first-order release constant; k<sub>H</sub> is the Higuchi release constant; k<sub>KP</sub> is the release constant incorporating structural and geometric characteristics of the drug- dosage form; n is diffusion release exponent.

## 862 List of figures

863 **Fig. 1** Liposome size distribution and polydispersity of ‘empty’ and EGCG loaded liposomes

864 Liposome size distribution and polydispersity, determined by DLS, comparing (A) ‘empty’  
865 and (B) EGCG loaded formulations with Tween 20 (0-10 % w/w). Liposomes were prepared  
866 by the dry film hydration method and EGCG added during the lipid mixing stage. Data  
867 represents mean  $\pm$  SD. n=3 independent batches. \*\*\*\* indicates statistical comparison  
868 between the size of liposome formulations with a  $P \leq 0.0001$ . # # indicates statistical  
869 comparison between the polydispersity of liposome formulations with a  $P \leq 0.01$ .

870 **Fig. 2** Entrapment efficiency of EGCG in liposomes formulated with 0-10% w/w Tween 20

871 Entrapment efficiency (%) of EGCG in liposomes formulated with varying amounts of  
872 Tween 20 (0-10% w/w) Data represents mean  $\pm$  SD. n=3 independent batches. \*\*\*\* indicates  
873 statistical comparison between the entrapment efficiency of liposome formulations with a  $P \leq$   
874 0.0001.

875 **Fig. 3** Deformability index for ‘empty’ and EGCG loaded liposomes

876 Deformability index following extrusion through 50 nm membranes for ‘empty’ and EGCG  
877 loaded liposomes with increasing surfactant loading up to a maximum of 10% w/w.  
878 Liposomes were prepared adapting the dry film method adding the surfactant and adding  
879 EGCG during the lipid mixing stage. The preparation was vortexed and then extruded through  
880 the membranes. Data represents mean  $\pm$  SD. n=3 independent batches. \*\*\*\* indicates  
881 statistical comparison between the DI of liposome formulations with a  $P \leq 0.0001$ .

882 **Fig. 4** Differential scanning calorimetry scan of EGCG

883 All experimental runs commenced at an initial temperature of 0 °C with a scan rate of 10  
884 °C/min to 300 °C. Peak a and b are related to the epimer of EGCG, GCG. Peak c represents  
885 the glass transition temperature ( $T_g$ ) of EGCG was at 220 °C and the melting point ( $T_m$ ) of  
886 EGCG was at 245 °C.

887 **Fig. 5** Differential scanning calorimetry analysis scans of PC, cholesterol and Tween 20 and  
888 EGCG blends

889 DSC analysis scans of (A) PC, cholesterol and Tween 20 blend and (B) PC, cholesterol,  
890 Tween 20 and EGCG blend. The  $T_m$  of the lipid mixture is 172 °C, and upon addition of  
891 EGCG, the  $T_m$  was 191 °C. All experimental runs started at an initial temperature of 0 °C,  
892 purged under nitrogen gas, with a scan rate of 10 °C/min to 300 °C.

893 **Fig. 6** *In-vitro* percentage EGCG cumulative release profiles from solution and liposomal  
894 formulations

895 EGCG release profiles from solution and liposomes formulated with 0, 2, 6 or 10 % w/w  
896 Tween 20 over 24 hours. Liposomes were prepared adapting the dry film method adding the  
897 surfactant and EGCG during the lipid mixing stage. A diffusion cell dialysis system was used  
898 to evaluate *in-vitro* drug release. Data represents mean  $\pm$  SD. n=3 independent batches. \*\*\*\*

indicates statistical comparison between the EGCG release of liposome formulations with a  $P \leq 0.0001$ .

**Fig. 7** Stability of EGCG loaded liposomes as determined by size

Size of EGCG loaded liposomes formulated with 0-10% w/w Tween 20, using DLS, formulated with up to 10% w/w Tween 20 measured on various days (1, 7, 14, 21 and 28). Data represents mean  $\pm$  SD. n=6 independent batches.

**Fig. 8** Liposome encapsulation efficiency for EGCG

Liposome encapsulation efficiency for EGCG in liposomes formulated with 2 % w/w Tween 20 liposomes over 28 days. Liposomes were prepared adapting the dry film method adding the surfactant and drug during the lipid mixing stage. The preparation was then washed via centrifugation. The quantity of EGCG in supernatant over 28 days was then analysed by HPLC coupled with UV detection to assess liposome stability. Data represents mean  $\pm$  SD. n=6 independent batches.

**Fig. 9** Cellular toxicity of EGCG

HDFa (A) and HaCat (B) cells were grown on a 96-well plate at a density of  $50 \times 10^3$  cells per well and exposed to various concentrations of EGCG (0.01-100  $\mu$ M) for 24 hours. Thereafter 25  $\mu$ L of a 12.5:1 parts mixture of XTT to menadione was added each well. Plates were incubated for 3 hours at 37°C and the absorbance read at 450 nm. Data is reported as mean  $\pm$ SD with 6 replicates per compound in at 3 independent experiments. \*\*\*\*, \*\*\*, \*\*, \* indicates statistical comparison between the entrapment efficiency of liposome formulations with a  $P \leq 0.0001$ , 0.001, 0.01 and 0.05 respectively.

**Fig. 10** Localisation of DilC labelled liposomes loaded with EGCG and 2% w/w Tween 20 in HaCat cells

Cells were grown on the coverslips for 2 days. Cell nuclei were visualised using (A) DAPI (Blue). Liposomes were formulated with DilC for visualisation (B) (yellow). Liposome localisation within the cell is shown in the merged image (C).

**Fig. 11** Localisation of DilC labelled liposomes loaded with EGCG and 2% w/w Tween 20 in HDFa cells

Cells were grown on the coverslips for 2 days. Cell nuclei were visualised using (A) DAPI (Blue). Liposomes were formulated with DilC for visualisation (B) (yellow). Liposome localisation within the cell is shown in the merged image (C).

**Word count: 10773**